KSME Journal, Vol. 1, No. 2, pp. 121~127, 1987.

INCOMPRESSIBLE LAMINAR FLOW NEAR A CORNER OF 90° ANGLE

Yong Kweon Suh* and Chun Kun Park*

(Received March 12, 1987)

Numerical integration is conducted for two-dimensional incompressible laminar flow over a 90° corner. Using Newton's method, the Navier-Stokes equations are generated up to $Re=2800$, with the result that the corner generates a second bubble near $Re=800$. There exist distinct patterns for the evolution of the pressure gradient and the position of a separation point. As Re is increased the pressure gradient tends to approach zero over the recirculated region and shows sharper variations near the separation and reattachment points. Thus, these results confirm the free streamline model for separation proposed by Sychev.

Key Words: Corner, Newton's Method, Second Bubble, Separation, Boundary Layer, Free Streamline Model.

NOMENCLATURE

i	: Index to denote the step number in ξ-direction
I	: i at the downstream edge $\xi=\xi_m$
j	: Index to denote the step number in η-direction
J	: j at $\eta=\eta_m$
M	: Jacobian for $z\rightarrow\rho$
p	: Non-dimensional pressure
Re	: Reynolds number
s	: Coordinate along the wall
w	: x_1+iy_1
x_1, y_1	: Coordinate system in w-plane
x, y	: Coordnate system in z-plane
x_s	: Separation point
z	: $x+iy$
ζ	: Vorticity
η	: Normal component of ρ
η_m	: Displacement thickness of the boundary layer flow over a wedge
η_m	: η at the upper edge
ξ	: Tangential component of ρ
ξ_m	: ξ at the downstream edge
ρ	: $\xi+i\eta$
T	: Wall shear defined as Eq.(14)
ψ	: Stream function
Ψ	: Eq.(6)
Ψ_m	: Ψ at $\eta=\eta_m$

1. INTRODUCTION

Steady laminar flow at high Reynolds numbers over a submerged obstacle is merely an academic problem, as in reality flows are rarely steady nor laminar at high Reynolds numbers. However, because it concerns the basic problem of the limiting solutions as $Re\rightarrow\infty$, this problem has received much attention. Most of the fundamental work regarding this problem has focussed on laminar flow over a circular cylinder. Until the 1970's, many numerical investigations (Dennis and chang, 1970 ; Son and Hanratty, 1969 ; Takami and Keller 1969 ; Patel, 1976) have revealed that the length of the wake bubble behind the circular cylinder increases as $O(Re^{\frac{1}{2}})$. Very recently, Fornberg (Fornberg, 1980 ; Fornberg, 1986) presented the numerical solutions of the Navier-Stokes equations for flows past a cylinder at Reynolds numbers up to 600. His remarkable finding was that the width of the wake begins to grow as $O(Re)$ from about $Re=400$. The large wake bubble consists mainly of a pair of vortices low and very uniform vorticity. The region between the cylinder and these vortices has nearly zero interior vorticity. His results for such a compatively large Reynolds number flow were made possible by the availability of a super computer, the use of the Newton's method, and a special treatment of the far-field boundary conditions.

On the other hand, little attention has been paid to flows with bubbles on the order of the body scale, such as flow over the forward-facing step, stagnation flow impinging on an infinite flat plate with a normally protruding finite flat plate (the present case), and flow over a trough, etc. In these cases, the separated regions will contain the body-scaled eddies at high Reynolds numbers. Intuitively, it is expected that growth of the bubble will be somewhat constrained by the inertia force of the oncoming inviscid flow. Therefore, features exhibited by this flow field will differ from those with large bubbles in the wake.

The purpose of this paper is to study (i) the structure of the flow field near the separation point and the reattachment point, and (ii) the various existing wake models for high -Reynolds-number flow past an obstacle.

2. THE GEOMETRY AND THE GOVERNING EQUATIONS

The geometry of the solid wall to be concerned in this paper consists of a finite flat plate and a semi-infinite flat

Department of Mechanical Engineering, Dong-A University, Pusan 600, Korea

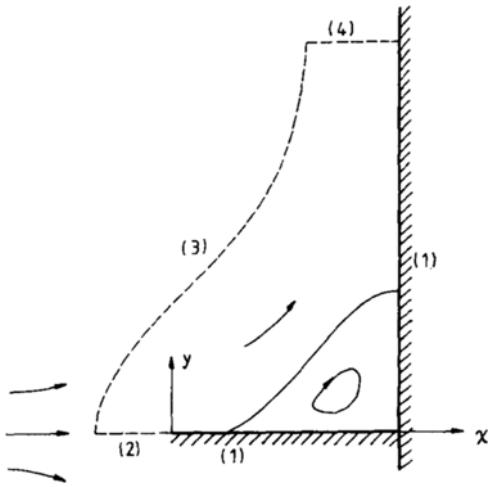

Fig. 1 Geometry of the problem and the boundary conditions in the z-plane; (1) No-slip; (2) Symmetry; (3) Inviscid; (4) Boundary layer

plate as shown in Fig. 1. Here, the length of the frontal plate is used to normalize the coordinates.

Because of the geometry, our analysis will be facilitated by a suitably chosen coordinate system. To incorporate all the local features, we introduce a two-step conformal mapping;

$$z \rightarrow w \rightarrow \rho \tag{1}$$

where

$$z=x+iy,\ w=x_1+iy_1,\ \rho=\xi+i\eta \tag{2}$$

$$w=1-(1-z)^2 \tag{3}$$

$$w=\rho^2 \tag{4}$$

The first mapping (3) is the so called Schwarz-Christoffel transformation and considers the flow pattern far from the corner in the inviscid zone. The transformation also allows the walls to be represented by the simple equation, $\eta=0$, $\xi>0$, so that the no-slip condition on the wall is simplified. The coordinates obtained by the second mapping (4) are the optimal coordinates (Kaplun 1954) incorporating the singular nature near the leading edge and the boundary layer flow farther downstream. In terms of stream function, ψ, and vorticity, ζ, the Navier-Stokes equations for steady, two-dimensional and incompressible flow in the z-plane can be written as

$$\nabla^2_{xy}\psi=\zeta,\quad \nabla^2_{xy}\zeta=Re\frac{\partial(\zeta,\ \psi)}{\partial\ (x,\ y)}$$

which can be coupled to yield in the ρ-plane:

$$\begin{aligned}\nabla^4\Psi&+\left[\frac{2}{M}\frac{\partial M}{\partial\eta}+2Re(\eta-\eta_w)\right]\frac{\partial}{\partial\eta}\nabla^2\Psi\\&+\left[\frac{2}{M}\frac{\partial M}{\partial\xi}-2Re\xi\right]\frac{\partial}{\partial\xi}\nabla^2\Psi+\left[\frac{1}{M}\nabla^2M+\frac{2Re}{M}\right.\\&\left.\frac{\partial M}{\partial\eta}(\eta-\eta_w)\right.\\&\left.-\frac{2Re}{M}\frac{\partial M}{\partial\xi}\xi\right]\nabla^2\Psi+Re\left[\frac{\partial\Psi}{\partial\xi}\frac{\partial}{\partial\xi}\nabla^2\Psi-\frac{\partial\Psi}{\partial\eta}\right.\\&\frac{\partial}{\partial\xi}\nabla^2\Psi\\&\left.+\left(\frac{1}{M}\frac{\partial M}{\partial\eta}\frac{\partial\Psi}{\partial\eta}-\frac{1}{M}\frac{\partial M}{\partial\xi}\frac{\partial\Psi}{\partial\eta}\right)\nabla^2\Psi=0,\right.\end{aligned}\tag{5}$$

where M is Jacobian for $z\rightarrow\rho$ and

$$\psi=2\xi(\eta-\eta_w)+\Psi, \tag{6}$$

where ψ is stream function. Here and henceforth, all the fluid properties are non-dimensionalized with respect to the suitable references. Re is based on the kinematic viscosity of the fluid, the length of the frontal plate, and the reference velocity; the reference velocity will be automatically defined in the course of the coordinate transformation (3). The first term of the right- hand side of (6) is the asymptotic solution of the boundary layer equation for large η and farther downstream from the origin, and $2\xi\eta_w$ represents the displacement thickness. Detailed discussion regarding (6) is made in (Suh, 1986). In other words, Ψ is a stream function perturbed from Hiemenz flow.

3. NEWTON'S METHOD FOR STEADY SOLUTIONS AND THE NUMERICAL SCHEME

Most numerical methods for solving the steady-state Navier-Stokes equations are either time-dependent or time-like in their iterations (Roache, 1975; Roache and Ellis, 1975). The primary diffeculties associated with these unsteady approaches are two-fold; the problem of stability and the problem of convergence. Newtons method is widely used in solving especially the nonlinear algebraic equations. Since the beginning of the 1980's, the idea of applying Newton's method to solve the Navier-Stokes equations numerically has appeared in a number of papers (Fornberg, 1980; Fornberg, 1986; Walter and Larsen, 1981). The rate of iterative convergence offered by Newton's method is quadratic and thus much faster than any other iterative scheme mentioned above. The main disadvantage of this so called "FON" method (the Fourth Order Newton' method named by Walther and Larsen (Walter and Larsen, 1981)) is that for a grid system of $I\times J$ with $J<I$, approximately $2\times I\times J^2$ variable storages are needed at the least. Depending on the type of machine, a supplementary memory system can be used; therefore, the CPU time wil be increased accordingly in writing and reading the data.

Another importnat factor involved in Navier-Stokes calculations is the implementation of the far-field boundary conditions. A detailed study made by Fornberg(Fornberg, 1980) showed that the influence of the far-field boundary conditions on the solution became more significant as Reynolds number was increased.

Until now there has not been a numerical solution of the Navier-Stokes equations for the incompressible corner flow. Leal's work (Leal, 1973), is for flow over a finite flat plate when the flow at a large distance is given by the stream function $\psi=xy$ and plate is situated on the x-axis from -1 to 1(Leal, 1973). Although the basic inviscid flow is the same as that over a 90° corner wall, the boundary conditions are different.

In the present study, we shall adopt the Newton's method to study the corner flow problem. It should be mentioned here that there are two regions which add difficulty to this prob-

lem ;areas near the leading edge and near the corner. As Re is increased, the boundary layer thickness becomes thinner, which requires finer step sizes in the streamwise direction near the leading edge. These finer step sizes allow for the adequate treatment of the abrupt change of the flow property in this region.

On the other hand, when the separation bubble appears near the corner it is widened and lengthened as Re is increased. Thus, even with the use of the Newton's method, the stability and accuracy of the solution is restricted by the boundary layer thickness, the size of the bubble and thus the Reynolds number.

Formal application of the Newton' s method to (5) yields.

$$A\Psi = B\bar{\Psi}, \tag{7}$$

where $\bar{\Psi}$ is the present value and Ψ is the one to be obtained. A and B are linear operators defined as

$$A=\frac{1}{Re}\nabla^4+P_1\frac{\partial}{\partial\eta}\nabla^2+P_2\frac{\partial}{\partial\xi}\nabla^2 +R\nabla^2+S_1\frac{\partial}{\partial\eta}+S_2\frac{\partial}{\partial\xi}, \tag{8}$$

$$B=\left(\frac{\partial\bar{\Psi}}{\partial\xi}\right)\frac{\partial}{\partial\eta}\nabla^2+\left(-\frac{\partial\bar{\Psi}}{\partial\eta}\right)\frac{\partial}{\partial\xi}\nabla^2 +\left(\frac{1}{M}\frac{\partial M}{\partial\eta}\frac{\partial\bar{\Psi}}{\partial\zeta}-\frac{1}{M}\frac{\partial M}{\partial\xi}\frac{\partial\bar{\Psi}}{\partial\eta}\right)\nabla^2. \tag{9}$$

$P_1, P_2, \ldots, S_2$ can be expressed in terms of M and Ψ [refer to (Suh, 1986) for detailed formula]. Boundary conditions of the present problem are as shown in Fig. 2. The boundary condition on (4) of Fig. 2 is based upon the bundary layer solution for Hiemenz flow. One of the boundary conditions on (3) of Fig. 2, i. e., $\zeta=0$, is clearly understood. As was mentioned by Fornberg (Fornberg, 1980), the conventional assumption $\Psi=0$ or $\frac{\partial^2\Psi}{\partial\eta^2}=0$ for the other boundary condition would bring forth significantly erroneous results, especially at high Reynolds number. The condition chosen in this study comes from the potential flow solution for the region outside of (3) of Fig. 2, and thus the problem of finiteness in the computational domain can be partially overcome.

The well known solution [refer to e.g. (Hildebrand, 1976)] of the inviscid equation

$$\nabla^2\Psi=0$$

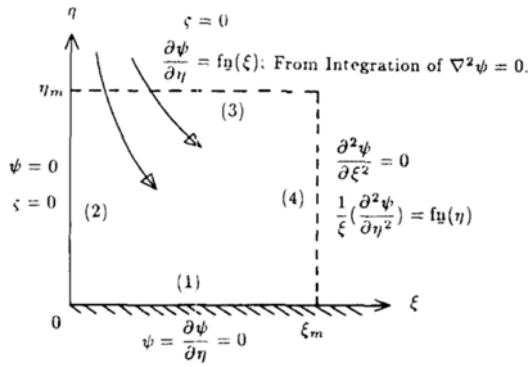

Fig. 2 Boundary conditions in the ρ-plane

for the inviscid zone [above (4) of Fig. 2] is

$$\Psi(\xi,\ \eta)=\frac{\eta-\eta_m}{\pi}\int_{-\infty}^{\infty}\frac{\Psi(t,\ \eta_m)}{(\xi-t)^2+\eta_1^2}dt \qquad (\eta_1=\eta-\eta_m). \tag{11}$$

Equation (11) is used to relate $\Psi(\xi, \eta_m+\nabla\eta)$ to five unknowns $\Psi(\xi, \eta_m)$ of the most adjacent mesh points and one unknown $\Psi(\xi_m, \eta_m)$; although the actual physical domain in ξ is infinite, as is also considered in (11), this must be cut for the computational domain at a suitable distance, i. e., $\xi=\xi_m$, where the boundary layer assumption is valid as a matter of accuracy. Here Ψ for $\xi>\xi_m$ is assumed to be of the same magnitude as Ψ at $\xi=\xi_m$ (Fornberg, 1986).

We define the column vectors $\phi_2,\ \phi_3,\ \cdots\ \phi_{I-1},\ \phi_I$ as

$$\phi_i=\begin{pmatrix}\Psi_{i,2}\\ \Psi_{i,3}\\ \vdots\\ \Psi_{i,J}\end{pmatrix} \qquad (i=2,\ 3,\ \cdots,\ I).$$

Then the appropriate finite difference formula for (7) and (11) can be represented by the block penta-diagonal matrix as follows;

$$\begin{bmatrix} A_{22} & A_{23} & A_{24} & 0 & 0 & \cdots & \cdots \\ A_{32} & A_{33} & A_{34} & A_{35} & 0 & 0 & \cdots \\ A_{42} & A_{43} & A_{44} & A_{45} & A_{46} & 0 & \cdots \\ 0 & A_{53} & A_{54} & A_{55} & A_{56} & A_{57} & 0 \\ \cdots & \cdots & \cdots & \cdots & \cdots & \cdots & , \\ 0 & \cdots & \cdots & 0 & A_{I-2,\ I-4} & A_{I-2,\ I-3} & A_{I-2,\ I-2} \\ 0 & \cdots & \cdots & \cdots & 0 & A_{I-1,\ I-3} & A_{I-1,\ I-2} \\ 0 & \cdots & \cdots & \cdots & \cdots & 0 & 0 \end{bmatrix}$$

$$\begin{bmatrix} \cdots & A_{21} \\ \cdots & A_{31} \\ \cdots & A_{41} \\ \cdots & A_{51} \\ \cdots & \cdots \\ A_{I-2,\ I-1} & A_{I-2,\ I} \\ A_{I-1,\ I-1} & A_{I-1,\ I} \\ A_{I,\ I-1} & A_{I,\ I} \end{bmatrix} \begin{pmatrix}\phi_2\\ \phi_3\\ \vdots\\ \vdots\\ \vdots\\ \phi_1\end{pmatrix} = \begin{pmatrix}Q_2\\ Q_3\\ \vdots\\ \vdots\\ \vdots\\ Q_1\end{pmatrix} \tag{12}$$

where Q_i is the load vector and all elements of the coeffecient matrix are $(J-1)\times(J-1)$ and diagonalized. Equation (12) is solved by the block unit using the Gaussian elimination method with partial pivoting. The computational process is apparent and it is repeated until a certain convergence criteria is met.

4. NUMERICAL RESULTS AND DISCUSSIONS

In the present study, we choose η_m to be fixed value

$$\eta_m=\frac{6}{\sqrt{2\times100}} \tag{13}$$

so that it can accomodate the growth of the bubble(s). Here η_m of (13) corresponds to the boundary layer edge for Hiemenz flow at $Re=100$, where 6 is measured by the normal component of the boundary layer coordinates. The coordinate system used throughout the calculation is shown in Fig. 3. We note that the leading edge singularity can be

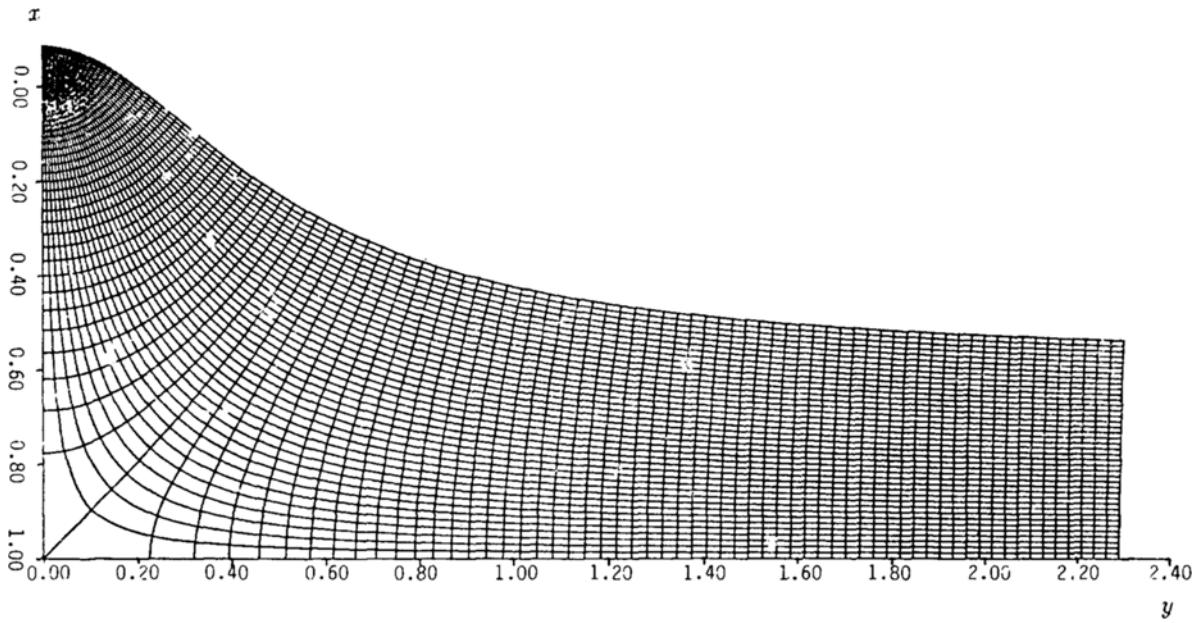

Fig. 3 The Mesh System : I=101, J=41

absorbed by the present system of coordinates, while the outer edge of the domain tends to follow the direction of the local flow so that there would be as few as possible unnecessary meshes over the domain. Nevertheless, problems still exist in the mesh system. Near the corner, the scale factor becomes infinitely large, and thus any discretization scheme with this mesh might fail to represent the detailed flow field of this small region. The initial Re was 100, with the boundary layer solution for the Hiemenz flow used as the initial value. It took only 5 itrations to attain the appropriate convergence limit for such relatively large recirculated flow as shown in Fig. 4(a). The solution for $Re=100$ is then used as the initial value in obtaining that for $Re=200$, and so on. The increment of Re is 100 up to $Re=800$, 200 up to $Re=1600$, and 400 up to $Re=2800$.

It seems that only several iterations are suffecient to achieve the desired convergence criteria. Shown in Fig. 4 through Fig. 6 are the levels of ψ and ζ for $Re=100$, 800,

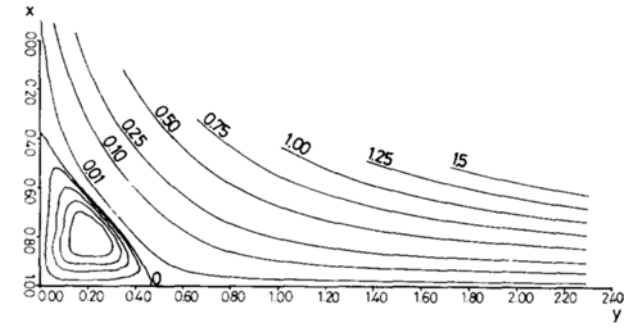

(a)

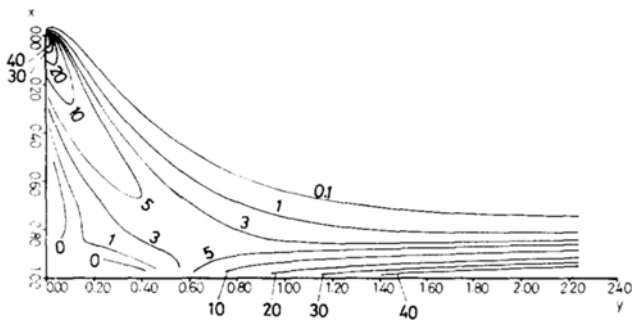

(b)

Fig. 4 ψ, ζ for $Re=100$: (a) ψ; (b) ζ

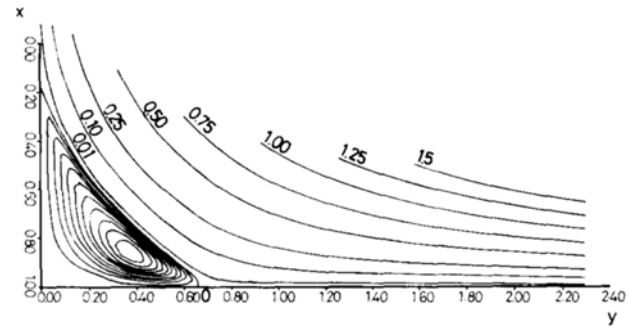

(a)

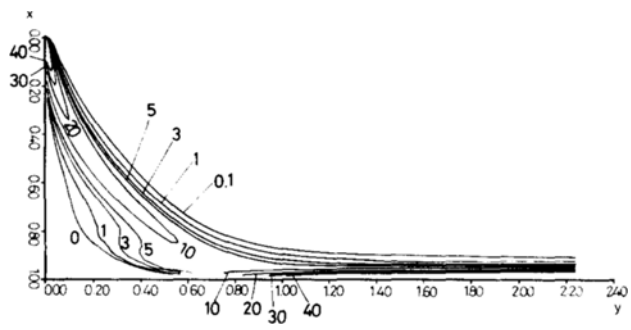

(b)

Fig. 5 ψ, ζ for $Re=800$: (a) ψ; (b) ζ

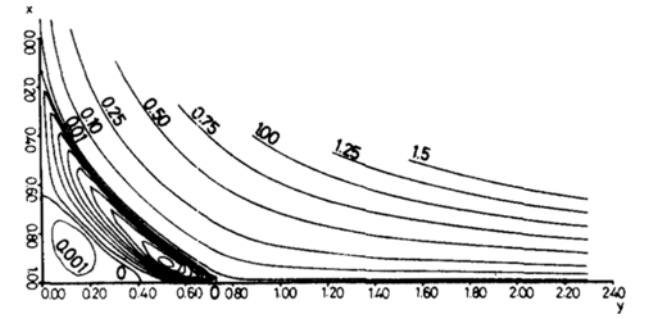

(a)

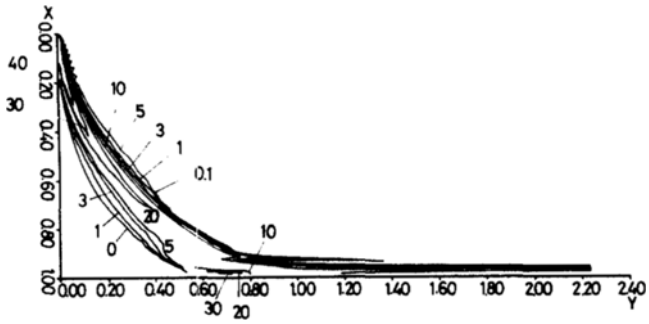

(b)

Fig. 6 ψ, ζ for $Re=2800$: (a) ψ; (b) ζ

2800, respectively. It is interesting to note from these results that the corner generates a second bubble at about $Re=800$, 2800, respectively. It is interesting to note from these results that the corner gennerate a second bubble at about $Re=800$. The second bubble turns out to have much slower motion of fluid particle and is more viscous than the first one as seen from Fig. 6(a) and (b). In addition, the growth of this bubble is faster than the first one. It seems that equi-vorticity lines tend to congregate especially on the bordering lines of the first bubble as Reynolds number is increased; this result then, seems to support the Prandtl-Batchelor model (Batchelor, 1956a; Batchelor, 1956b) where it is assumed that the bubble coinsists of constant vorticity. These results also suggest that at higher Reynolds number, the thickness of the first bubble will decrease due to the faster growth of the second one. Furthermore, we note that the vortex center of the first bubble moves toward the wall $x=1$ as Re is increased. This movement can also be seen in Fig. 7, where the magnitude of wall shear

$$\tau=\frac{1}{2\sqrt{2Re}\,\xi}\left[\frac{\partial^2\psi}{\partial\eta^2}\right]_{\eta=0}$$
$$\begin{cases}\tau\to 0.46960\cdots\text{(Blasius)} \\ \quad \text{as } \xi\to 0 \\ \tau\to 1.23258\cdots\text{(Hiemenz)} \\ \quad \text{as } \xi\to\infty\end{cases} \tag{14}$$

on the upstream surface decreases and that on the downstream surface increases as Re is increased. Consequently, it is likely that the first bubble will break down into two smaller ones. The bubble in the downstream region will be smaller in size but have stronger vortex intensity than the one in the upstream region. It is further conjectured that the corner will generate more bubbles as Re is increased. Unfortunately, the range of Re for the present study is not sufficient to verify these trends.

The pressure gradient $\frac{\partial p}{\partial s}$ is given as

$$\frac{\partial p}{\partial s}=\frac{1}{Re}\left(\frac{|1-\xi|^{\frac{1}{2}}}{\xi}\right)^3\frac{\partial^3\Psi}{\partial\eta^3} \tag{15}$$

where

$$\frac{\partial^3\Psi}{\partial\eta^3}=\frac{\Psi_{i,3}-4\Psi_{i,2}+\xi(6\eta_w-4\nabla\eta)}{\nabla\eta^3}$$

where s is the distance along the wall from the leading edge. For various values of Re, this pressure gradient is shown in Fig. 8. It is interesting to note that as Re is increased the pressure gradient tends to zero over the recirculated region and changes more rapidly at the separation point near the leading edge and at the reattechment point downstream. A similar but indistinctive trend was also observed by Leal (Leal, 1973). This trend, of course, supports the idea of the free streamline theory in which the pressure in the recirculated region is assumed to be constant. Concerning the rapid change in the pressure gradients at the separation point (and reattachment point), we resort to detailed study of the flow structure around the separation point. Based on the asymptotic behavior of the free streamline pressure gradient, Sychev (Sychev, 1972) showed that at large Re, separation takes place under the action of a large local positive pressure gradient, which becomes infinite like $O(Re^{\frac{1}{8}})$ as Re is in-

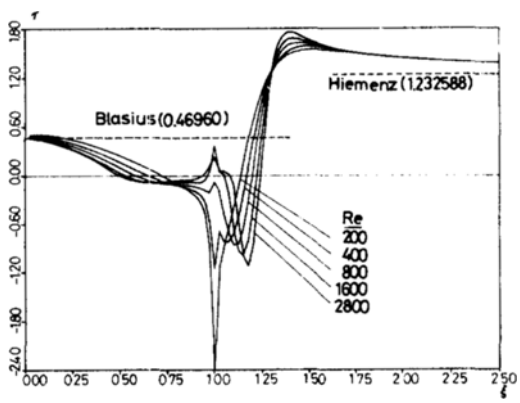

Fig. 7 Distribution of the wall shear

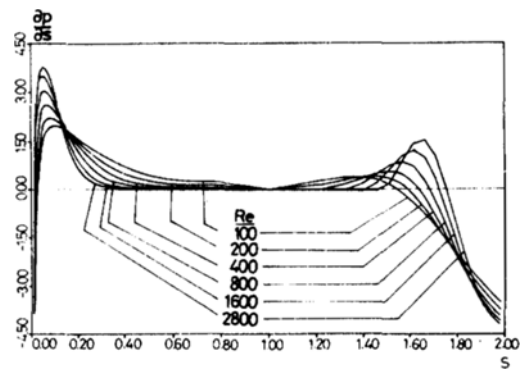

Fig. 8 Distribution of the pressure gradient

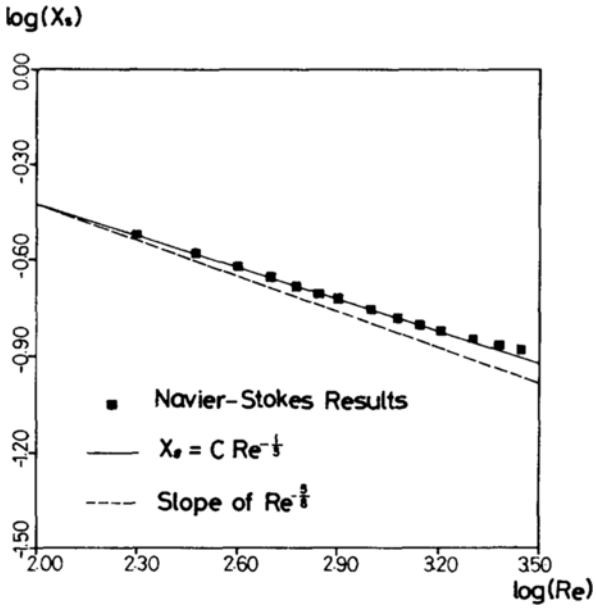

Fig. 9 Dependence of x_s upon Re

creased. The extent of the region over which this pressure gradient has an effect tends to zero as $Re^{-\frac{3}{8}}$; essentially, the structure of Sychev's model in the neighborhood of the separation point is the same as that of the triple deck theory [refer to (Smith, 1982) for the element of the triple deck]. However, Sychev's model made it possible to reconcile the inviscid breakaway (the classical jet theory) and the viscous separation (the boundary layer separation) [refer to (Smith, 1979) for the reconciliation problem]. It is then of interest to observe whether or not there would exist enough room ahead of the separation point such that the boundary layer could develop over that region. The location of the separation point, x_s, measured from the leading edge, is plotted in Fig. 9 against Re. It is seen that x_s can be represented by

$$X_s \cong C\ Re^{-\frac{1}{3}} \tag{16}$$

where $C=1.\ 7445$. Since the order of x_s is higher than that of the interaction zone $Re^{-\frac{3}{8}}$ in Sychev's model, our present study seems to lend further support for the free streamline model of separation at high Reymolds numbers.

5. SUMMARY AND CONCLUSIONS

In this paper, the Navier-Stokes equations are solved numerically using Newton's method. The forth order partial differential equation for ψ is used instead of the ψ-ζ system of equations. One of the boundary conditions at the upper edge of the domain ($\eta=\eta_m$) is supplied from the integration of the inviscid equation in $\eta \geq \eta_m$ with the boundary condition $\Psi = \Psi_m$ at $\eta = \eta_m$. For the mesh system $I \times J$, the centered difference scheme yields $(I-1)\times(J-1)$ equations. Using the appropriate vector notation, this set of equations is reduced to a matrix form where the coeffecient matrix is a penta-diagonal and each element block matrix is also diagonalized. The value of Ψ for $\zeta \geq \zeta_m$ is assumed to be the same as that at $\zeta=\zeta_m$, and is treated as one of the unknowns. The Gauss elimination method is then applied to solve the coeffecient matrix in the block unit. The invese of the block matrix is obtaind with the aid of the Gaussian elimination method with partial pivoting for stability and accuracy. Back substitution then follows to give new values of Ψ.

For a 90° corner solutions are obtained for Re up to 2800. The results indicate that a second bubble begins to appear at approximate $Re=800$. This second bubble grows faster than the first one, thus causing the first one to become thinner. As Re is increased, the pressure gradient tends to zero along the wall surface in the recirculated region, and the rapid change in the pressure gradient is confined to narrower regions near the separtion point and the reattachment point. The point of separation is simply represented by the formula (16) and thus approaches the leading edge like $O(Re^{-\frac{1}{3}})$. The present results thus seem to confirm the free streamline model for separation proposed by Sychev.

REFERENCES

Batchelor, G.K., 1956a, "On Steady Laminar Flow with Closed Stream Lines at Large Reynolds Number", JFM, Vol. 1, pp. 177~190.

Batchelor, G.K., 1956b, "A Proposal Concerning Laminar Wakes behind Bluff Bodies at Large Reynolds Number", JFM, Vol. 1, pp. 388~398.

Dennis, S.C.R. and Chang, G.Z., 1970, "Numerical Solutions for Steady Flow past a Circular Cylinder at Reynolds Numbers up to 1000", JFM, Vol. 42, pp. 471~485.

Fornberg, B., 1980, "A Numerical Study of Steady Viscous Flow past a Circular Cylinder", JFM, Vol. 98, pp. 819~855.

Fornberg, B., 1986, "Steady Viscous Flow past a Circular Cylinder up to Reynolds Number 600", J. Comp. Phys., Vol. 61, pp. 297~320.

Hildebrand, F. B., 1976, Advanced Calculus for Applications, second ed., Prentice-Hall, Inc., Englewood Cliffs, N. J., U.S.A., pp. 473~474.

Kaplun, S., 1954, "The Role of Coordinate Systems in Boundarylayer Theory", ZAMP, Vol. 5, pp. 111~135.

Leal, L. G., 1973, "Steady Separated Flow in Linearly Decelerated Free Stream", JFM, Vol. 59, pp. 513~535.

Patel, V.A., 1976, "Time-Dependent Solutions of the Viscous Incompressible Flow Past a Circular Cylinder by the Method of Series Truncation", Computers and Fluids, Vol. 4, pp. 13~27.

Roache, P. J., 1975, "The LAD, NOS, and Split NOS Methods for the Steady-State Navier-Stokes Equations", Computers and Fluids, Vol. 3, pp. 179~195.

Roache, P.J. and Ellis, M.A., 1975, "The BID Method for the Steady-State Navier-Stokes Equations", Computers and Fluids, Vol. 3, pp. 305~320.

Smith, F. T., 1979, "Laminar Flow of an Incompressible Flow past a Bluff Body: The Separation, Reattachment, Eddy Properties and Drag", JFM, Vol. 92, pp. 171~205.

Smith, F.T., 1982, "On the High Reynolds Number Theory of Laminar Flow", IMA J. Appl. Math., Vol. 28, pp. 207~281.

Son, J.S. and Hanratty, T. T., 1969, "Numerical Solution for the Flow around a Circular Cylinder at Reynolds Numbers of 40, 200 and 500", JFM, Vol. 35, pp. 369~386.

Suh, Y. K., 1986, "On Laminar Viscous Flow over a Corner", Ph. D. Dissertation, State Univ. of New York at Buffalo,

Buffalo, NY, U.S.A.

Sychev, V. V., 1972, "Laminar Separation", Fluid Dynamics, Vol. 7, pp, 407~417.

Takami, H. and Keller, H., 1969, "Steady Two-Dimensional Viscous Flow of an Incompressible Fluid Past a Circular Cyliner", High-speed of Computing in Dynamics, The Physics of Fluids Supplement II, pp. 51~56.

Walter, K. T. and Larsen, P.S., 1981, "The FON Method for the Steady-State Two-Dimensional Navier-Stokes Equations", Computers and Fluids, Vol. 9, pp. 365~376.